Supporting Information for the Manuscript

Conformational analysis of oligomeric aggregation intermediate states of an immunoglobulin light chain protein

Tejaswini Pradhan,[a,b] Riddhiman Sarkar,[a,b] Nadine Schwierz,[c] Martin Zacharias,[d] and Bernd Reif [a,b]*

[a] Bayerisches NMR Zentrum (BNMRZ) at the Department of Chemistry, Technische Universität München (TUM), Lichtenbergstr. 4, 85747 Garching, Germany

[b] Helmholtz-Zentrum München (HMGU), Deutsches Forschungszentrum für Gesundheit und Umwelt, Institute of Structural Biology (STB), Ingolstädter Landstr. 1, 85764 Neuherberg, Germany

[c] Institute of Physics, Computational Biology, University of Augsburg, Universitätsstraße 1, 86159 Augsburg, Germany

[d] Institute of Protein Biochemistry, Ulm University, Helmholtzstr. 8/1, 89081 Ulm, Germany

[e] Medical Department V, Amyloidosis Center, Heidelberg University Hospital, 69120 Heidelberg, Germany.

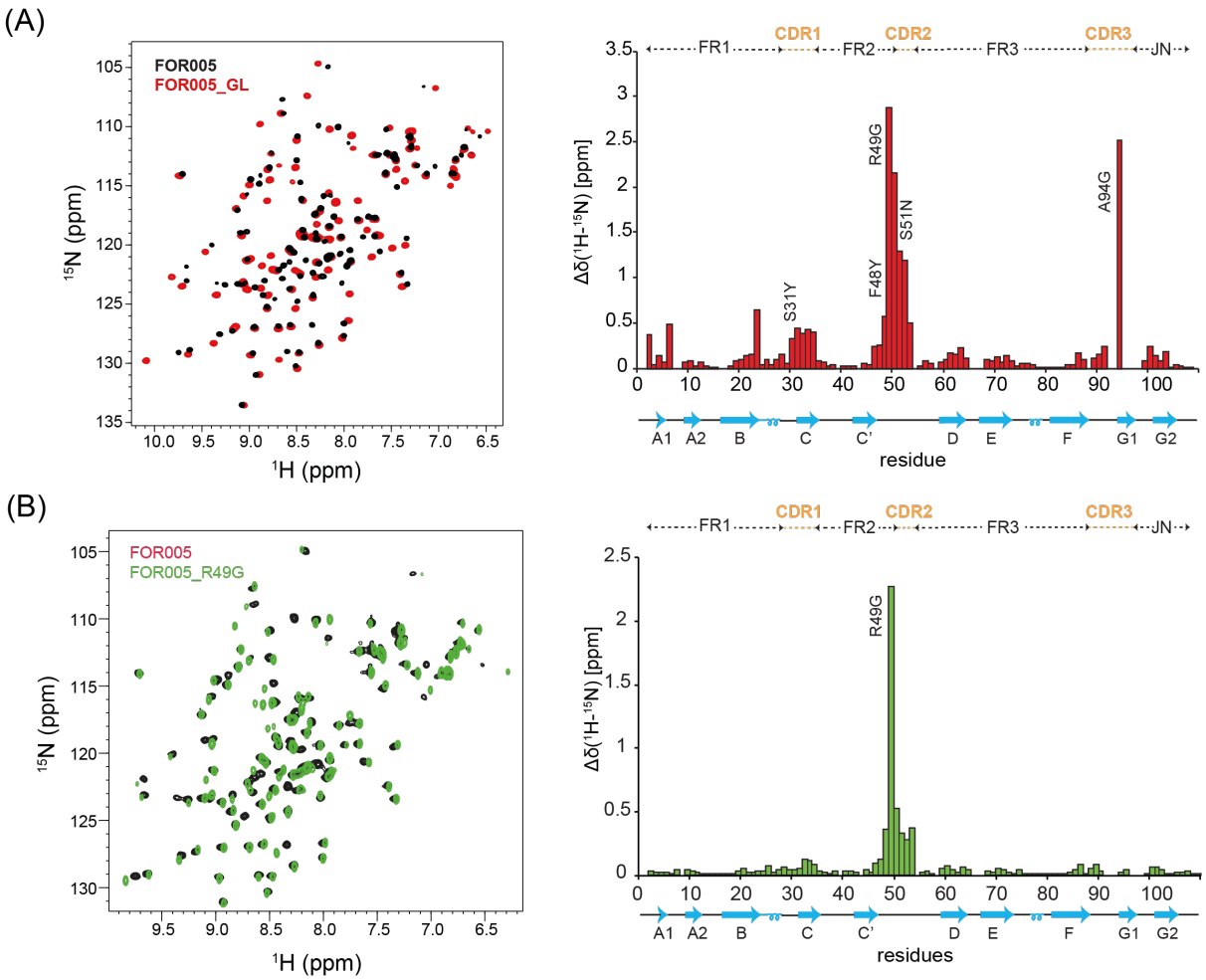

Figure S1. *^{1}H,^{15}N HSQC spectra and chemical shift differences between FOR005 patient and variant proteins.* (A) *Chemical shift perturbations of the FOR005 patient protein in comparison to GL. ^{1}H,^{15}N HSQC of FOR005 in black are superimposed with spectra of GL shown in red. (B) Chemical shift perturbations of the FOR005 patient protein in comparison to the single point mutant FOR005-R49G. Mutations from patient to germline (and patient to FOR005-R49G) are indicated in the chemical shift histograms.*

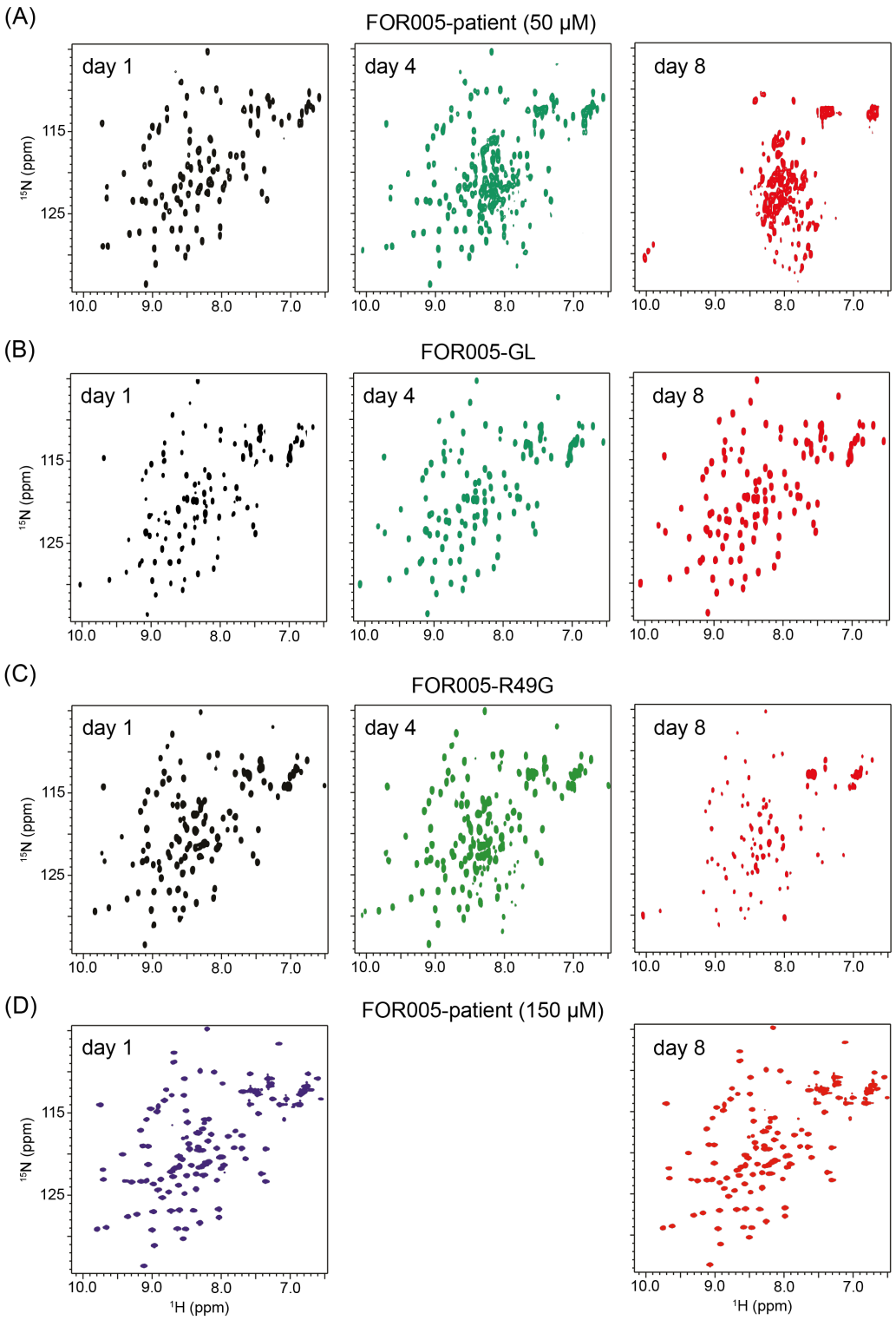

Figure S2. *Aggregation kinetics of different FOR005 variants followed by solution state NMR HSQCs. Superposition of $^{1}H,^{15}N$ HSQC spectra acquired over a period of 1 week for a 50 µM sample of FOR005 (A), GL (B) and R49G (C). All experiments were recorded at a temperature of 25°C. For FOR005, new peaks become visible after a period of 3 days which indicate protein unfolding. For GL, no additional cross peaks appear in the spectra over time. For R49G, a few new peaks are observed in the course of the experiment. (D) Superposition of $^{1}H,^{15}N$ HSQC spectra recorded at day 1 (blue) and day 8 (red) for FOR005 at a protein concentration of 150 µM. Under these conditions, no aggregation is observed.*

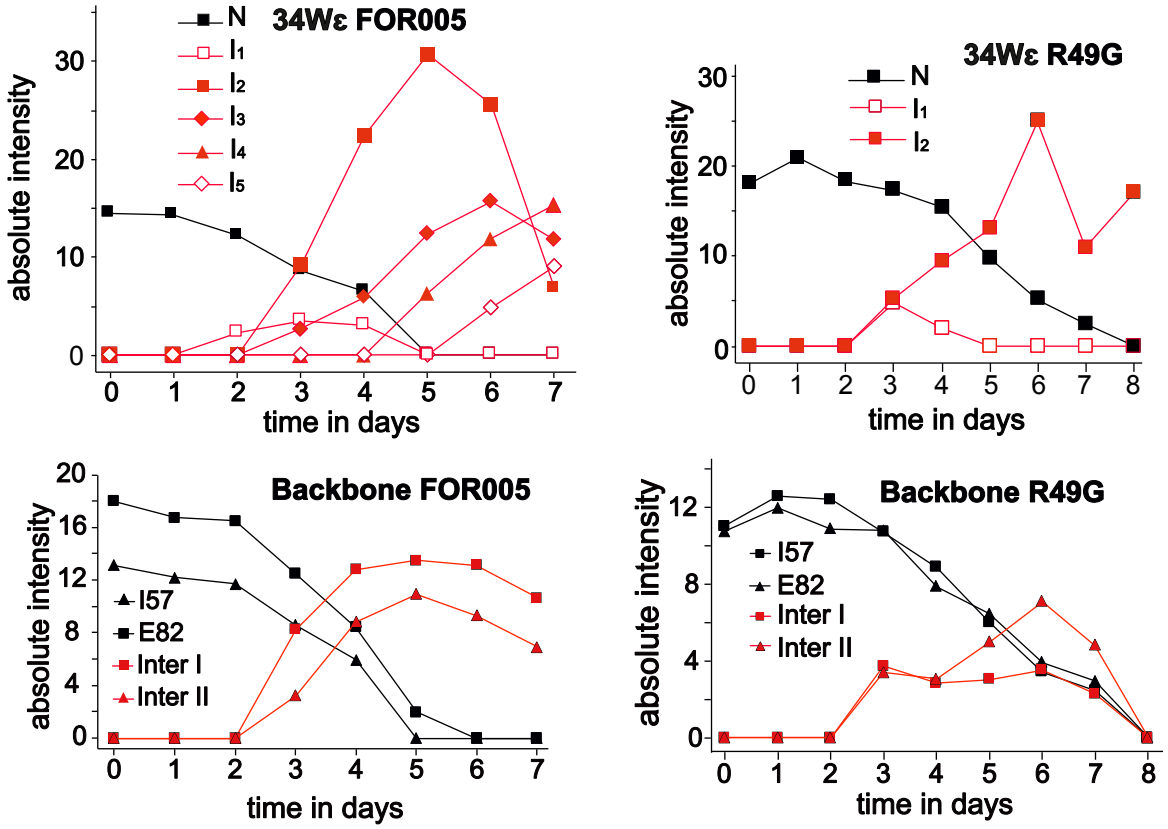

Figure S3. *(Top) W34ε cross peak intensity as a function of time for FOR005 and R49G. (Bottom) Backbone cross peak intensities as a function of time for FOR005 and R49G.*

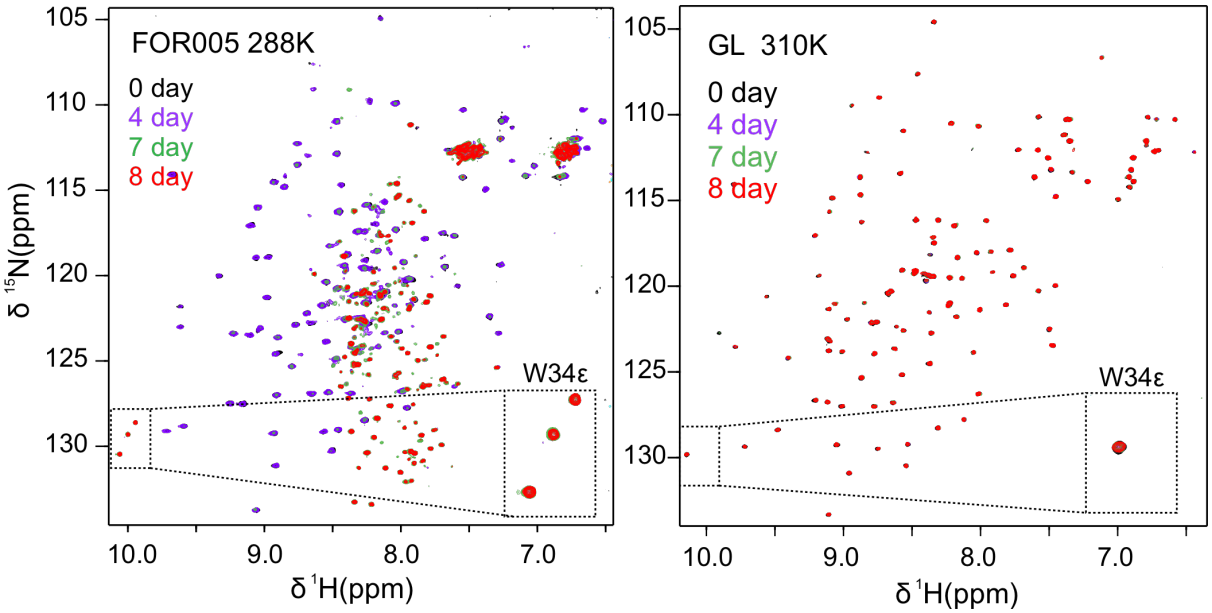

Figure S4. *Superposition of the $^{1}H,^{15}N$ HSQC spectra obtained for FOR005 and GL recorded at 288 K and 310 K respectively as a function of time. A concentration of 50 μM for both proteins was used in the experiments.*

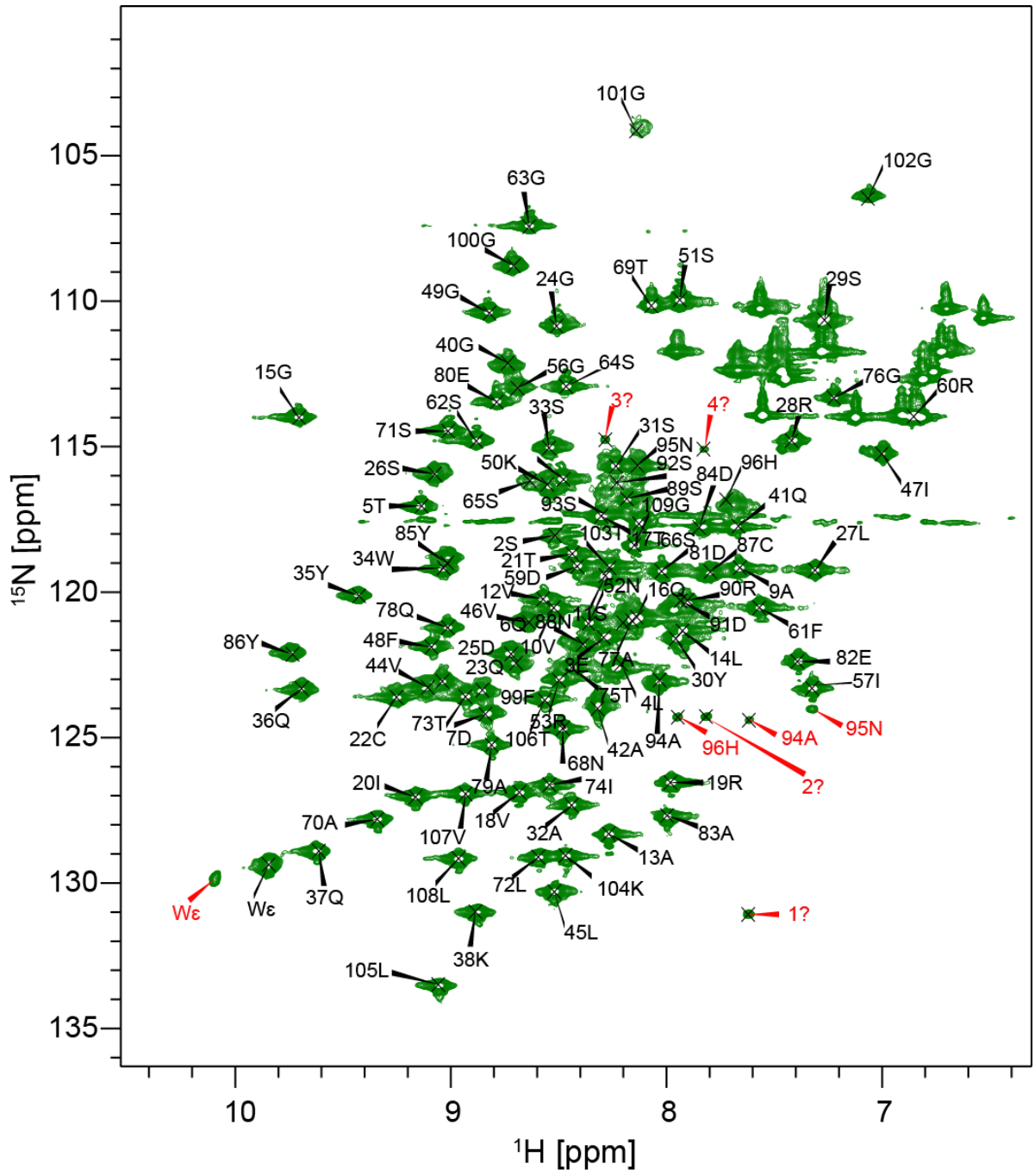

Figure S5. *$^{1}H,^{15}N$ HSQC spectrum obtained for FOR005-R49G obtained after several weeks. A protein concentration of 700 µM was employed in the experiment.*

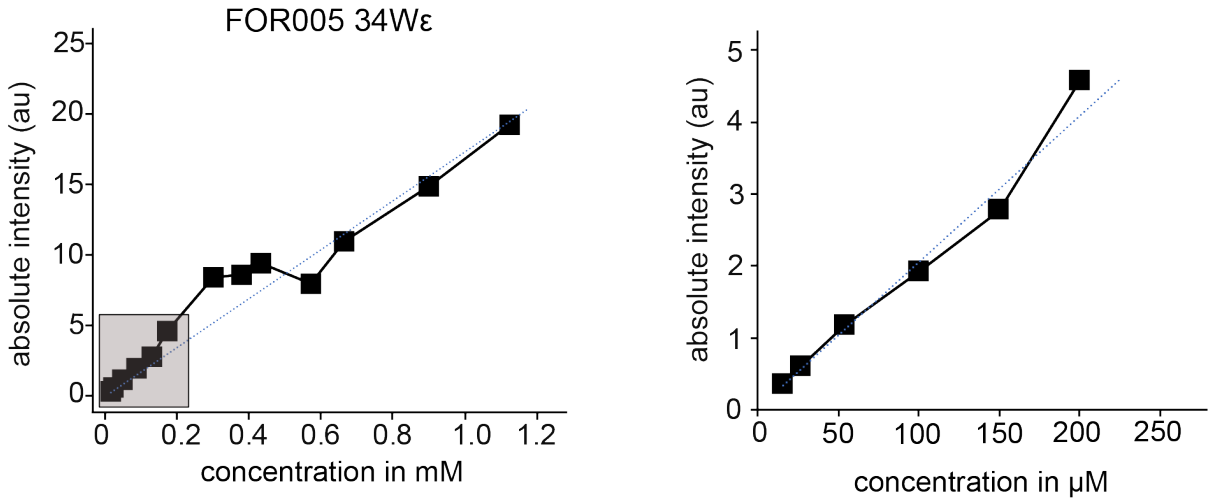

Figure S6. *(A) Correlation between absolute signal intensity and sample concentration for the W34ε side chain resonance in the native state. The intensity was extracted from concentration dependent $^{1}H,^{15}N$ HSQC spectra. The plot on the right represents the grey shaded region enlarged.*

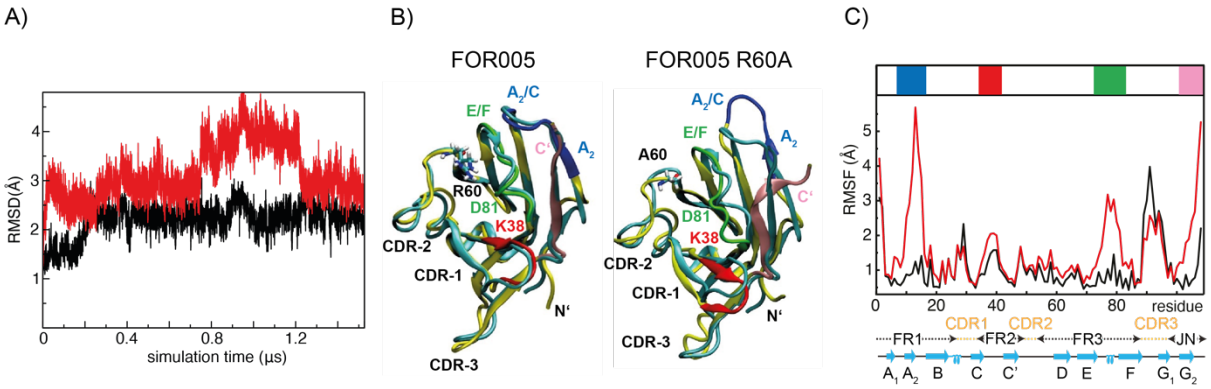

Figure S7. *Molecular dynamics simulations of the patient protein FOR005 and the single point mutant R60A. (A) The simulation was carried out in explicit solvent for a duration of 1.6 µs. (B) Superposition of the backbone structures for FOR005 and FOR005 R60A for a snapshot in the simulation at t=0 and t=1 ns. (C) Root-mean-square fluctuations (RMSF) as a function of residue calculated from the MD trajectory (1.6 µs, at 310 K) for the patient sequence FOR005 and the single point mutant FOR005-R60A. The color code on top of the figure highlights regions in the protein that become dynamic as a consequence of the point mutation R60A, and match the color of particular secondary structure elements in (B).*

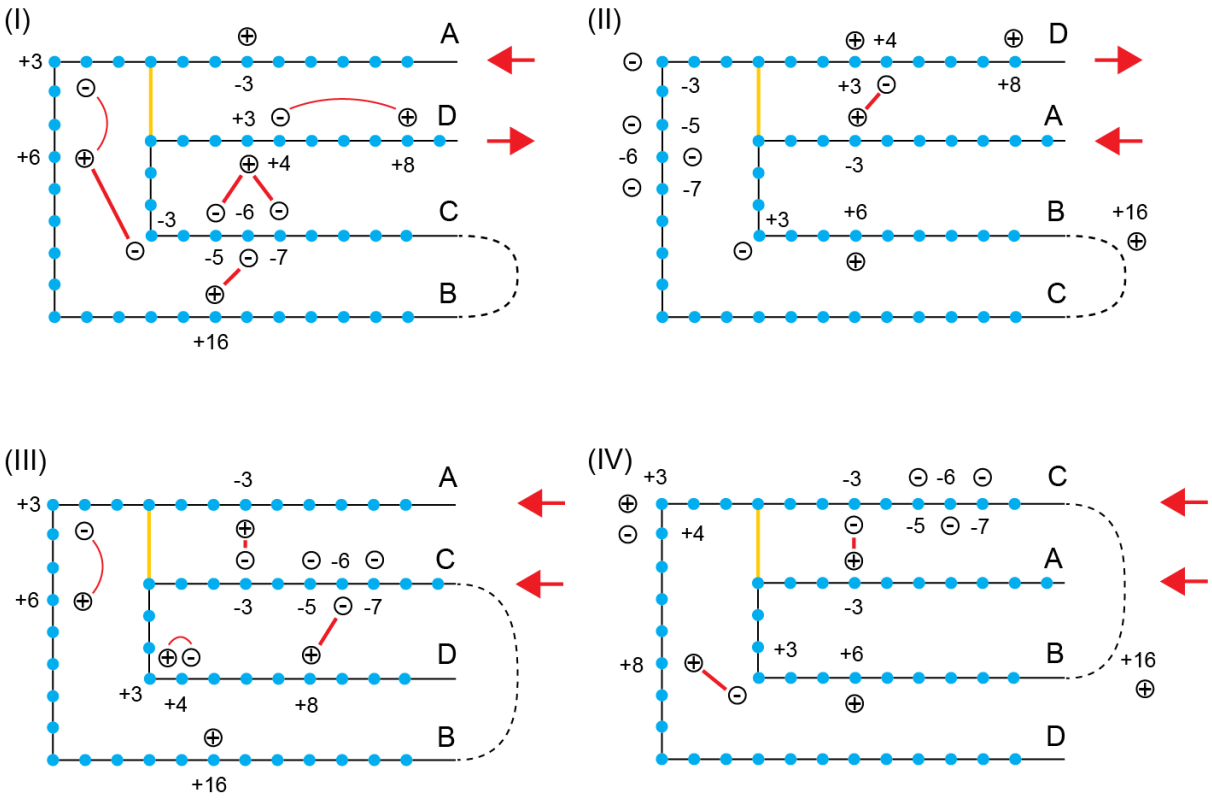

Figure S8. *Fibril topologies after reshuffling of strands around the most amyloidogenic strand A. Strands are named A, B, C, D according to their position with respect to the disulfide bond. In total, there are 4 possible arrangements. Strands A and B can be either positioned on the surface, while strands C and D are located in the core, or the reverse. In addition, the two inner strands can be reshuffled. (I) Experimental topology in the cryo-EM structure of FOR005 (Radamaker et al., 2021). The position of every charged amino acid is indicated relative to the disulfide. In this topology, every charged side chain is compensated with an opposite charged residue in the core of the amyloid fibril structure. Strands A/B and C/D are arranged in an antiparallel fashion. (II) Topology after exchange of the outer (A/B) and inner strands (C/D) (in comparison to topology I). A shift of the disulfide does not yield a charge compensation and retains a frustrated structure. This topology is thus not favorable. (III) Topology after reshuffling of the two inner strands C and D (in comparison to topology I). Strands A/B and C/D are arranged in parallel. In parallel strands, a shift of the disulfide does not result in a different arrangement of the charged side chains. The loop connecting strands B and C interferes with the C-terminus and thus yields a non-favorable topology. (IV) Topology after reshuffling of the outer strands C and D (with respect to topology II). Strands A/B and C/D are arranged in parallel. The loop connecting strands B and C interferes with the N-terminus and thus yields a non-favorable topology.*